Proc. Natl. Acad. Sci. USA
Vol. 88, pp. 8686–8690, October 1991
Biophysics

Cholesterol-induced fluid-phase immiscibility in membranes

(magic-angle spinning NMR/biradicals/hydrogen bonding/^{13}C relaxation rates)

MANTRIPRAGADA B. SANKARAM AND THOMAS E. THOMPSON

Department of Biochemistry, University of Virginia Health Sciences Center, Charlottesville, VA 22908

Communicated by Saul Roseman, July 3, 1991

ABSTRACT **The fluid-phase behavior of binary mixtures of cholesterol with phosphatidylcholines is investigated using magnetic resonance methods. Phospholipid biradicals provide the electron spin resonance spectroscopic resolution of two immiscible fluid phases in the dipalmitoylphosphatidylcholine–cholesterol system. Isotropic chemical shifts of the phospholipid carbonyl carbons in binary mixtures with cholesterol measured using solid-state high-resolution nuclear magnetic resonance methods furnish evidence for a putative hydrogen bond between the 3β-hydroxyl of cholesterol and the *sn*-2 carbonyl of the phospholipid. The location in the bilayer of cholesterol in the two fluid phases is determined by measuring spin label-enhanced spin–lattice relaxation rates of the ^{13}C nuclei of both the phospholipid and cholesterol molecules. These results suggest, in a time-averaged sense, that in the cholesterol-poor fluid phase the cholesterol molecule essentially spans the bilayer, whereas in the cholesterol-rich fluid phase the molecule is present in both monolayers of the bilayer.**

A number of studies on two-component, two-phase lipid bilayers and monolayers have examined conditions under which two immiscible phases coexist (1, 2). Interest has centered on the size, shape, and connectivity of the phase domain structure in these systems. The characteristics of this domain structure are functions of temperature, pressure, and chemical composition and reflect the interactions between the component lipid molecules. In almost all cases studied the two coexisting phases in phospholipid bilayers have been solid/solid or fluid/solid. This has been the case also for cholesterol–phospholipid systems (3–5). However, recent work has called to attention the coexistence of two immiscible fluid phases in phospholipid bilayers containing cholesterol (6–9).

The phase diagram for the 1,2-dipalmitoyl-*sn*-glycero-3-phosphocholine (DPPC)–cholesterol multilamellar lipid bilayers is shown in Fig. 1*B*. The phase diagrams for mixtures of cholesterol with other phospholipids, differing in both the acyl chain and the headgroup composition, have the same overall shape and consist of three one-phase regions and two two-phase regions as shown in Fig. 1*B* (8). The phases are denoted solid-ordered (s_o), liquid-ordered (ℓ_o), and liquid-disordered (ℓ_d). In the two-phase regions there is coexistence of the s_o and ℓ_o phases or of the two fluid phases, ℓ_d and ℓ_o. The occurrence of fluid-phase immiscibility has been suggested by a triphasic dependence on cholesterol concentration of the hyperfine interactions of phospholipid spin labels incorporated into cholesterol-containing phospholipid bilayers (6, 8).

In this communication, we present magnetic resonance evidence further substantiating cholesterol-induced fluid-phase immiscibility and suggesting the existence of hydrogen bonding between cholesterol and phospholipid molecules. We conclude by proposing a bilayer model specifying the time-averaged location of cholesterol in the ℓ_d and ℓ_o phases.

The publication costs of this article were defrayed in part by page charge payment. This article must therefore be hereby marked "*advertisement*" in accordance with 18 U.S.C. §1734 solely to indicate this fact.

MATERIALS AND METHODS

Materials. Unlabeled phospholipids were purchased from Avanti Polar Lipids (Birmingham, AL). Phospholipid monoradicals and ^{13}C-enriched phospholipids were synthesized as described (8). The biradical was synthesized by acylation of *sn*-glycero-3-phosphocholine with the corresponding fatty acid spin labels (11).

ESR Spectroscopy. The ESR spectra were recorded on an X-band Varian E-line spectrometer. The sample preparation protocols and the details of instrumentation are as described earlier (8). The monoradical spin label concentrations used were 1 mol % unless otherwise specified. The biradical concentrations were 0.5 mol %.

NMR Spectroscopy. ^{13}C NMR spectra were recorded at 90 MHz on a Nicolet NT-360B spectrometer equipped with a variable-temperature magic-angle spinning probe from Doty Scientific (Columbia, SC). The samples contained in zirconium rotors were spun at speeds between 1 and 3 kHz, which yielded spectra free from rotational side bands. The spin–lattice relaxation times were measured by the 180-τ-90 inversion-recovery pulse sequence.

RESULTS AND DISCUSSION

Spectroscopic Resolution of the ℓ_d and ℓ_o Phases. Fig. 2 shows the ESR spectra of a phosphatidylcholine monoradical spin labeled at the 16th position in the *sn*-2 chain, 1-stearoyl-2-[16-(4,4-dimethyloxazolidine-*N*-oxyl)stearoyl]-*sn*-glycero-3-phosphocholine (16-doxyl-PC), and of a phosphatidylcholine biradical spin labeled at the 16th position in both the *sn*-1 and the *sn*-2 chains, 1,2-di-[16-(4,4-dimethyloxazolidine-*N*-oxyl)stearoyl]-*sn*-glycero-3-phosphocholine (di-16-doxyl-PC) (see Fig. 1*A*), incorporated into DPPC–cholesterol mixtures in the ℓ_d and the ℓ_o phases. The monoradical spectra reflect the well-known effect of a stronger cholesterol-induced motional restriction of the phospholipid molecules in the ℓ_o phase relative to the ℓ_d phase. The biradical preparation was found to contain a small proportion of the monoradical as clearly revealed in spectrum d in Fig. 2. The spectra of the biradical in the ℓ_d and the ℓ_o phases, from which the experimental monoradical spectra were subtracted, are shown in Fig. 2, spectra e and f, respectively.

The spectrum of the biradical in the ℓ_d phase (Fig. 2, spectrum e) corresponds to a singlet state for a spin-1/2 system, with the ^{14}N hyperfine interaction giving rise to the three lines. The three lines are strongly broadened both by dipole–dipole and by exchange spin–spin interactions between the two nitroxides. In contrast, the ESR spectrum of

Abbreviations: DPPC, 1,2-dipalmitoyl-*sn*-glycero-3-phosphocholine; 16-doxyl-PC, 1-stearoyl-2-[16-(4,4-dimethyloxazolidine-*N*-oxyl)stearoyl]-*sn*-glycero-3-phosphocholine; di-16-doxyl-PC, 1,2-di-[16-(4,4-dimethyloxazolidine-*N*-oxyl)stearoyl]-*sn*-glycero-3-phosphocholine.

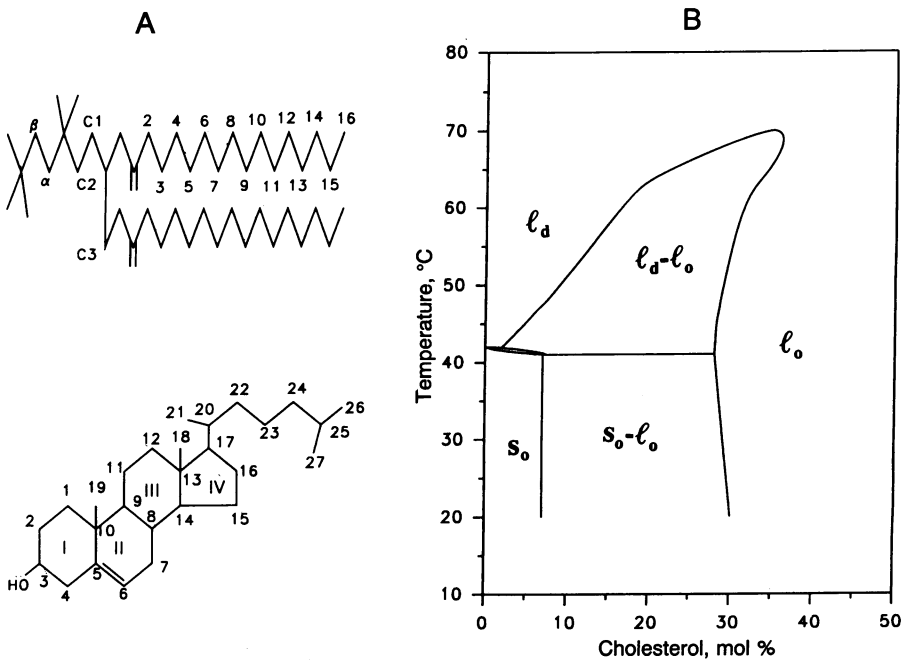

FIG. 1. (*A*) Chemical structures showing carbon numbering of DPPC (*Upper*) and cholesterol (*Lower*). (*B*) Temperature–composition phase diagram of the DPPC–cholesterol system. Experimental data from differential scanning calorimetry (3, 4, 10), x-ray diffraction (5), ^{2}H NMR spectroscopy (10), and spin-label ESR spectroscopy (6, 8) and statistical thermodynamic considerations (7) were used to obtain this phase diagram. See the text for a description of the phases.

the biradical in the ℓ_o phase (Fig. 2, spectrum f) is typical of a triplet state (12). In addition to any magnetic interaction present in the monoradical, there is a new interaction in the case of the biradical, which is the coupling between the two electron spins. For flexible biradicals the scalar and anisotropic components of this interaction are influenced by their surroundings, which modulate the molecular conformation and interspin separation (12). For the biradical situated in the anisotropic environment of the interior of phospholipid bilayers, the line widths and the separation between the two outermost lines in its ESR spectrum are determined by the distance between, and the dynamics of, the two nitroxide groups. Spectrum f in Fig. 2 must therefore be a result of the acyl chain condensing effect of cholesterol, which brings the two acyl chains in a phospholipid molecule closer together to increase dipole–dipole interactions (12). The separation between the two electron spins, r, may be estimated if it is assumed that the interacting spins are point dipoles and that the interaction is dipolar in nature. In this point-dipole approximation, r is related to the maximum separation between the two broad lines, d, by the expression $d = 55.6 \times 10^3 \times r^{-3}$ (13). The maximum separation, d, was obtained by recording the spectrum of the biradical in multilayers oriented on stacked glass plates with the plates oriented parallel to the pole faces of the magnet. The value of d at 20°C for an equimolar mixture of DPPC–cholesterol was 67 ± 5 G, which corresponds to an intramolecular interspin (and hence interchain) separation of 13.8 ± 1.1 Å. This is an increase of 3–4 Å in the interspin separation estimated for cholesterol-free DPPC bilayers.

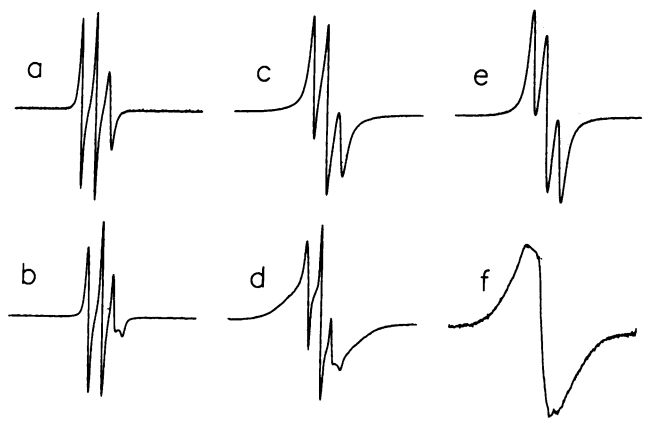

FIG. 2. ESR spectra of the di-16-doxyl-PC monoradical and of the di-16-doxyl-PC biradical in DPPC–cholesterol mixtures in the ℓ_d (5 mol % cholesterol) and in the ℓ_o (50 mol % cholesterol) phase at 60°C. Spectrum a, 16-doxyl-PC in a DPPC–cholesterol mixture in the ℓ_d phase; spectrum b, 16-doxyl-PC in a DPPC–cholesterol mixture in the ℓ_o phase; spectrum c, di-16-doxyl-PC in a DPPC–cholesterol mixture in the ℓ_d phase; spectrum d, di-16-doxyl-PC in a DPPC–cholesterol mixture in the ℓ_o phase; spectrum e, the monoradical spectrum (spectrum a, 8% double-integrated intensity) was subtracted from spectrum b; spectrum f, the monoradical spectrum (spectrum b, 8% relative intensity) was subtracted from spectrum d. Spectral width = 200 G.

The Fluid-Phase Coexistence Region. The ESR spectra of the di-16-doxyl-PC biradical in DPPC–cholesterol in the ℓ_d–ℓ_o phase coexistence region consist of two resolved components as, for example, shown in Fig. 3*A* (spectrum a, solid line). One component is closely similar to the ℓ_d phase spectrum (spectrum b, solid line). The other component is characterized by the broad peaks in the outer wings of the spectrum and is similar to the ℓ_o phase spectrum (spectrum c, solid line).

The ℓ_d and the ℓ_o phase component spectra in the experimental spectra from the ℓ_d–ℓ_o phase coexistence region can be quantitated by difference and addition spectroscopy, as illustrated in Fig. 3*A*. Subtraction of the ℓ_o phase spectrum (c, solid line) from spectrum a (solid line) yields an ℓ_d phase spectrum (b, dashed line). The complementary subtraction of the ℓ_d phase spectrum (b, solid line) yields an ℓ_o phase spectrum (c, dashed line). Alternatively, the addition of the ℓ_o phase spectrum (c, solid line) to the ℓ_d phase spectrum (b, solid line) gives a two-component spectrum (a, dashed line) that corresponds very closely to the original experimental spectrum (a, solid line). Both the subtractions and the addition yield consistent results for the fractions of the ℓ_d and the

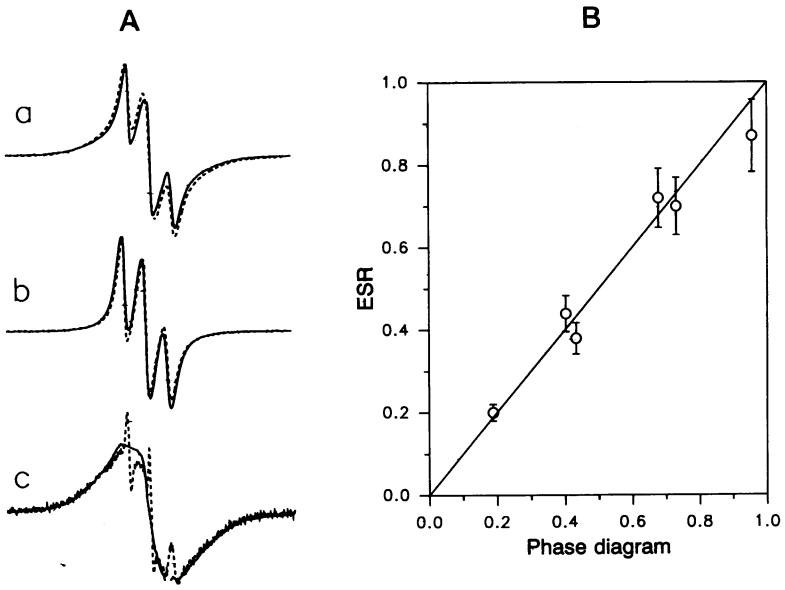

FIG. 3. (*A*) Spectral subtraction and addition with the di-16-doxyl-PC biradical. Solid lines are original experimental spectra at 60°C with the monoradical impurity spectrum subtracted: spectrum a, DPPC–cholesterol mixture in the ℓ_d–ℓ_o mixed-phase region with 25 mol % cholesterol; spectrum b, DPPC–cholesterol mixture in the ℓ_d phase with 5 mol % cholesterol; spectrum c, DPPC–cholesterol mixture in the ℓ_o phase at 50 mol % cholesterol. Dashed lines are summed or difference spectra: spectrum a, 60% ℓ_d phase spectrum plus 40% ℓ_o phase spectrum; spectrum b, ℓ_d–ℓ_o mixed phase spectrum minus 40% ℓ_o phase spectrum; spectrum c, ℓ_d–ℓ_o mixed phase spectrum minus 60% ℓ_d phase spectrum. Spectral width = 200 G. (*B*) Correspondence between the fractions of the ℓ_d phase in the ℓ_d–ℓ_o phase coexistence region determined from quantitative difference spectroscopy (ordinate) and those determined by the application of the lever rule to the phase diagram (abscissa) shown in Fig. 1*B*. The solid line is the expected behavior for exact correspondence.

ℓ_o phase component spectra at different cholesterol concentrations and temperatures. As shown in Fig. 3*B*, the fractions of the ℓ_d phase in the mixed-phase region as determined from spectroscopy are in good agreement with those obtained from the phase diagram.

The ESR spectra of the biradical in the ℓ_o, the ℓ_d, and the ℓ_d–ℓ_o regions for mixtures of cholesterol with glycerophospholipids containing different headgroups and acyl chains, and with sphingomyelins, are similar to those described above for DPPC (data not shown). The phase behavior of the binary mixtures of cholesterol with these phospholipids is qualitatively similar to that for the DPPC–cholesterol system (Fig. 1*B*). In addition, biradical positional isomers with the nitroxide groups at the 5, 7, or 12 positions gave results similar to the di-16-doxyl-PC label (data not shown). It thus seems highly unlikely that the spectral changes arise solely from the presence of the spin label group, but rather that they reflect fluid-phase immiscibility.

Cholesterol–Phospholipid Hydrogen Bonding. The effect of 50 mol % cholesterol on the isotropic chemical shifts of the phospholipid carbonyl carbons was studied by solid-state high-resolution ^{13}C NMR methods with magic-angle spinning. Spectra a and b in Fig. 4 are from DPPC alone and from an equimolar DPPC–cholesterol mixture in the ℓ_o phase, respectively. The presence of cholesterol induces a splitting in the otherwise single resonance by causing one of the

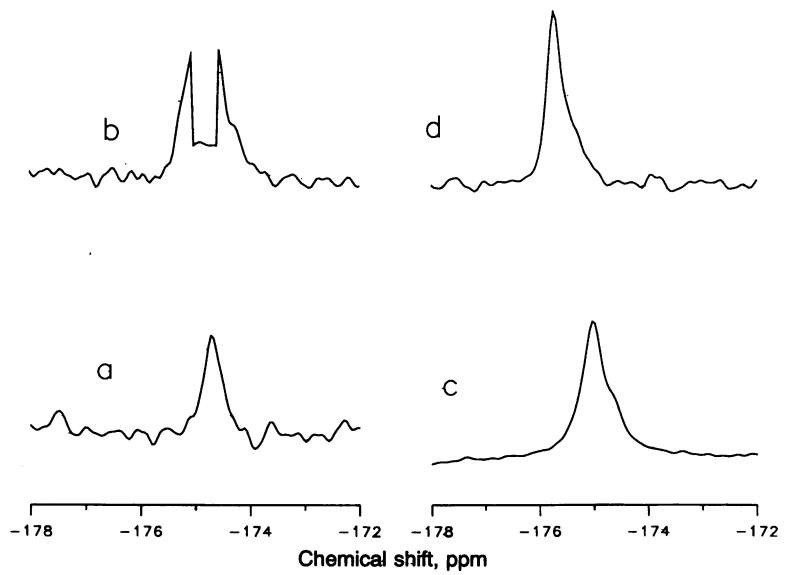

FIG. 4. Ninety-megahertz ^{13}C magic-angle spinning NMR spectra for the carbonyl carbon region of equimolar DPPC–cholesterol mixtures at 50°C. Spectrum a, DPPC alone; spectrum b, DPPC–cholesterol equimolar mixture; spectrum c, *sn*-2 carbonyl ^{13}C-enriched DPPC alone; spectrum d, equimolar mixture of ^{13}C-enriched DPPC and cholesterol.

carbonyl carbons to shift downfield by about 0.6 ppm at 50°C. A similar but somewhat smaller downfield shift has been reported (14) for an equimolar DPPC–cholesterol mixture dispersed in ^2H_2O. In order to assign the downfield-shifted signal to one of the two carbonyls, DPPC with the *sn*-2 carbonyl enriched in ^{13}C was examined. The NMR spectra of this compound are shown in spectra c and d in Fig. 4. In the presence of cholesterol, the *sn*-2 carbonyl carbon signal is shifted downfield, providing the assignment of the downfield signal to this carbon. This downfield shift is most probably due to a hydrogen bond between the 3β-hydroxyl of cholesterol and this carbonyl carbon. This conclusion is further supported by our observations that 50 mol % cholesterol induces a splitting of the two carbonyl carbons whether or not the samples are hydrated and by the fact that the chemical shift difference is essentially the same whether the dispersions are prepared in water (cf. Fig. 4) or deuterium oxide (14).

Location of Cholesterol in the ℓ_o Phase Bilayer. The presence of a spin label enhances the relaxation rates of the neighboring carbons (15–18). This effect was used to determine the location of cholesterol relative to that of a phospholipid spin labeled at the fifth position in the *sn*-2 chain. The spin label-enhanced relaxation rates, ΔR_{1z}, of the phospholipid carbons in the ℓ_o phase determined in a DPPC–cholesterol mixture containing 50 mol % cholesterol are shown in Fig. 5*A*. The largest effect of the spin label is seen for the carbonyl carbon, the acyl chain methylene carbons 2, 3, and 4, and for some of the carbons in the 5–13 range (see Fig. 1*A*). Although it is difficult to estimate the number and identity of the carbon atoms in the 5–13 range that are affected by the presence of the spin label at the fifth position, these data clearly show that the bilayer location of the phosphatidylcholine spin label is the same as that of the host DPPC. Shown in Fig. 5*B* are the ΔR_{1z} values of the cholesteryl carbons measured from the same set of ^{13}C NMR spectra as those used to obtain the data in Fig. 5*A*. In this case, the largest effect of the spin label occurs for carbons belonging to rings I and II. This observation suggests that these two rings are in the vicinity of the spin label. Since the relaxation rates of both the phospholipid and cholesterol carbon resonances were measured on the same spectrum, the phospholipid data provide an internal control because the spin label is a phospholipid derivative.

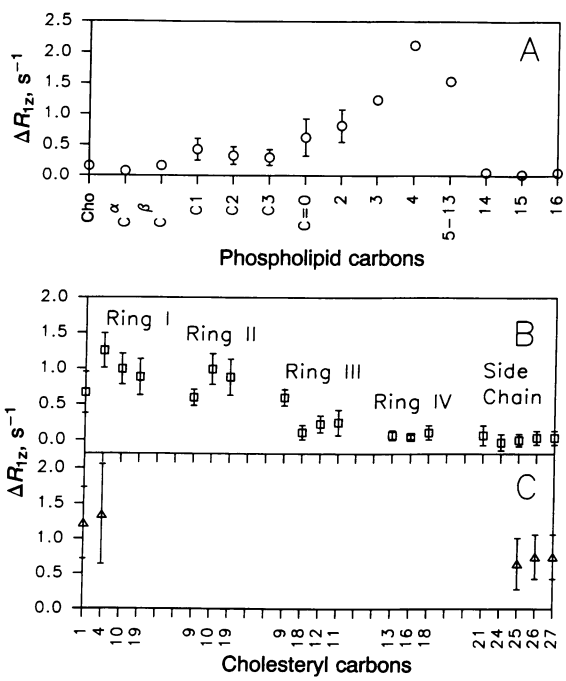

FIG. 5. (*A*) Spin label-enhanced spin–lattice relaxation rates, ΔR_{1z}, of the ^{13}C nuclei of DPPC at 50°C in the ℓ_o phase of a DPPC–cholesterol mixture at an equimolar ratio. ΔR_{1z} is the difference in relaxation rates in the presence and absence of the spin label. The spectral assignments of the phospholipid and cholesterol carbons are according to ref. 14 (see Fig. 1*A*). The concentration of 5-doxyl-PC was 1 mol %. (*B*) ΔR_{1z} values of the ^{13}C nuclei of cholesterol at 50°C in the ℓ_o phase. Only the resonances that correspond to single carbon assignments are considered since only these relaxation rates can be determined unambiguously. The concentration of 5-doxyl-PC was 1 mol %. (*C*) ΔR_{1z} in the ℓ_d phase. The total ^{13}C-enriched cholesterol was 5 mol % with respect to DPPC (2.5 mol % each of [3,4-^{13}C]cholesterol and [25,26,27-^{13}C]cholesterol). The concentration of 5-doxyl-PC was 5 mol %. Cho, choline.

Location of Cholesterol in the ℓ_d Phase Bilayer. The ℓ_d phase occurs at low cholesterol concentrations where no cholesteryl ^{13}C signals are visible in the NMR spectrum at natural abundance. Therefore, we used cholesterol enriched in ^{13}C at positions 3 and 4 and also enriched at positions 25–27 (see Fig. 1*A*). The ΔR_{1z} values in the ℓ_d phase using enriched cholesterol mixtures are shown in Fig. 5*C*. While carbons 3 and 4 show ΔR_{1z} values comparable to those in the ℓ_o phase, carbons 25, 26, and 27 on the flexible end of cholesterol show significantly larger enhanced rates. This suggests that both ends of the cholesterol molecule are in the vicinity of the fifth position of the phospholipid acyl chain and that ring I is closer to the fifth position than to the flexible end.

Molecular Organization in the ℓ_o and ℓ_d Phases. The information described above on the hydrogen bonding interactions between the cholesterol and the phospholipid molecules and the location of cholesterol can be interpreted in terms of different time-averaged molecular organizations in the ℓ_d and ℓ_o fluid phases. These are shown in Fig. 6. In the ℓ_d phase (Fig. 6*B*), the time-averaged position of cholesterol is transbilayer. Acyl chain lengths for this system determined using ^2H order parameters (19) suggest that, when the hydroxyl group is anchored at the carbonyl group by a hydrogen bond, the other end extends approximately up to carbon 8 of the phospholipid in the apposing monolayer. A more efficient packing of the cholesterol molecule can be achieved by a kink conformation in the phospholipid acyl chain, which has the correct dimensions to accommodate the flexible end of this steroid (20).

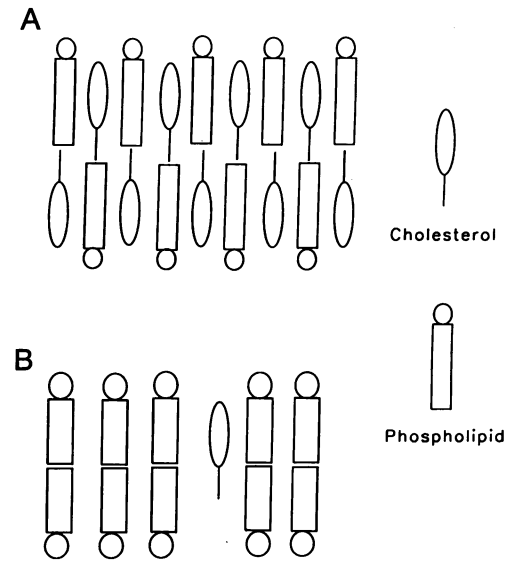

FIG. 6. Structural diagram depicting the distribution of the cholesterol and the phospholipid molecules in the transbilayer dimension. (*A*) The ℓ_o phase for an equimolar mixture. (*B*) The ℓ_d phase. See the text and ref. 19 for additional details.

In the ℓ_o phase (Fig. 6*A*), the relaxation rate data are consistent with a time-averaged organization in which the cholesterol molecules are present in both monolayers. Acyl chain lengths determined by ^{2}H NMR in this phase suggest that the hydrophobic thickness of the lipid bilayer is much larger than the ≈20-Å-long cholesterol molecule and that the average acyl chain length in each leaflet is significantly shorter than the length of cholesterol (19). The steroid must, therefore, penetrate partway into the other monolayer. Similarly, if the acyl chains are longer than the cholesterol molecule, then a part of the phospholipid molecule must extend beyond the midpoint of the bilayer. Such an arrangement leads to a model in which the hydrophobic ends of the cholesterol and the phospholipid molecules do not meet at the center of the bilayer, a mode of packing similar to that found in interdigitated lipid bilayer systems (21, 22).

We thank Dr. Jeff Ellena for his expert advice and assistance with the NMR experiments and Dr. Zhao-Qing Wang for the synthesis of the spin labels. We also thank Drs. Rodney Biltonen, Ching-hsien Huang, and Derek Marsh for useful suggestions and comments. This work was supported by Grant GM-14628 from the National Institutes of Health.

1. Vaz, W. L. C., Melo, E. C. C. & Thompson, T. E. (1989) *Biophys. J.* **56**, 869–876.
2. McConnell, H. M. (1990) *J. Phys. Chem.* **94**, 4728–4731.
3. Estep, T. N., Mountcastle, D. B., Biltonen, R. L. & Thompson, T. E. (1978) *Biochemistry* **17**, 1984–1989.
4. Mabrey, S., Mateo, P. L. & Sturtevant, J. M. (1978) *Biochemistry* **17**, 2464–2468.
5. Engelman, D. M. & Rothman, J. E. (1972) *J. Biol. Chem.* **247**, 3694–3697.
6. Recktenwald, D. J. & McConnell, H. M. (1981) *Biochemistry* **20**, 4505–4510.
7. Ipsen, J. H., Karlström, G., Mouritsen, O. G., Wennerström, K. & Zuckermann, M. J. (1987) *Biochim. Biophys. Acta* **905**, 162–172.
8. Sankaram, M. B. & Thompson, T. E. (1990) *Biochemistry* **29**, 10670–10675.
9. Wu, S. H. W. & McConnell, H. M. (1975) *Biochemistry* **14**, 847–852.
10. Vist, M. R. & Davis, J. H. (1990) *Biochemistry* **29**, 451–464.
11. Mason, J. T., Broccoli, A. V. & Huang, C. (1981) *Anal. Biochem.* **113**, 96–101.
12. Luckhurst, G. R. (1976) in *Spin Labeling Theory and Applications*, ed. Berliner, L. J. (Academic, New York), pp. 133–181.
13. Hirota, N. & Weissman, S. I. (1964) *J. Am. Chem. Soc.* **86**, 2538–2545.
14. Forbes, J., Bowers, J., Shan, X., Moran, L., Oldfield, E. & Moscarello, M. A. (1988) *J. Chem. Soc. Faraday Trans. 1* **84**, 3821–3849.
15. Levine, Y. K., Birdsall, N. J. M., Lee, A. G. & Metcalfe, J. C. (1972) *Biochemistry* **11**, 1416–1421.
16. Godici, P. E. & Landsberger, F. R. (1974) *Biochemistry* **13**, 362–368.
17. Ellena, J. F., Archer, S. J., Dominey, R. N., Hill, B. D. & Cafiso, D. S. (1988) *Biochim. Biophys. Acta* **940**, 63–70.
18. Brûlet, P. & McConnell, H. M. (1975) *Proc. Natl. Acad. Sci. USA* **72**, 1451–1455.
19. Sankaram, M. B. & Thompson, T. E. (1990) *Biochemistry* **29**, 10676–10684.
20. Huang, C.-H. (1977) *Lipids* **12**, 348–356.
21. Slater, J. L. & Huang, C. H. (1988) *Prog. Lipid Res.* **27**, 325–359.
22. Huang, C.-H. (1990) *Klin. Wochenschr.* **68**, 149–165.